

High-Quality Single Image 3D Facial Shape Reconstruction via Robust Albedo Estimation

Suwoong Heo*, Hyewon Song*, Jiwoo Kang* and Sanghoon Lee*[†]

* Department of Electrical and Electronic Engineering, Yonsei University, Seoul, South Korea

[†] Department of Radiology, College of Medicine, Yonsei University, Seoul, South Korea

E-mail: {heartshape, shw3164, jwkang, slee}@yonsei.ac.kr, Tel: +82-2-2123-2767

Abstract—In this paper, we present a method for high-quality single image 3D facial shape reconstruction with robust albedo estimation by using a prior face model. Motivated by the state-of-the-art methods for single image-based face reconstruction using the Shape from Shading (SfS), we develop a 3D facial recovery framework with innovative components. Specifically, rather than using the mean albedo, we use an optimized albedo of the 3D Morphable Model (3DMM) as a prior albedo model. In addition, we develop a robust weighting method based on the chromaticity of input and back-projected images. Combining these approaches produces a more robust albedo estimation which directly enhances the result of the SfS process. By using the tetrahedron-based deformation technique, a detailed facial shape can be accurately recovered from a single image. We demonstrate that our 3D facial recovery framework can reconstruct fine geometric details for a single image and outperforms the state-of-the-art in single image face reconstruction.

I. INTRODUCTION

The 3D face reconstruction, which is the process of inferring the 3D geometry of a human face model from 2D images, is the most fundamental core for applications such as face recognition [1], [2], 3D human pose estimation [3], [4], [5], [6], [7], face animation [8], [9], and so on. Especially, it is essential technology of the high-quality 3D human avatar generation for improving the quality of experience in virtual reality (VR) applications [10], [11].

There are several studies that attempted to reconstruct the 3D face model from a single image by optimizing the linear space parameters of the 3D Morphable Model (3DMM) [12], [13], [14], [15]. Rather than reconstructing 3D geometry based on stereo-matching [16] or deep-learning method without prior information [17], these methods are preferred because of it is applicable for in-the-wild images. However, those methods can only reconstruct the smooth parts of facial geometry except for the high-frequency details such as beard, pore, and wrinkles. For this reason, several methods have been proposed to recover high-frequency parts from the smooth geometry by using the Shape from Shading (SfS) [18], [19], [20], [21]. Specifically, these methods reconstruct the 3D face from a single image by using a two-step approach - recovering the smooth facial geometry by using 3DMM, and then enhances the facial details by using the SfS method. In [22], it is demonstrated that this strategy is effective for enhancing geometric details of a face from coarse facial geometry generated by the template face model.

Although this process could reconstruct the semantic parts

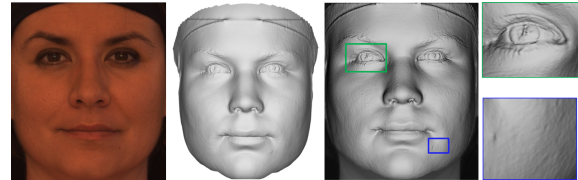


Fig. 1: For a given single image, the proposed method reconstructs a high-quality 3D facial shape by using the proposed robust albedo estimation.

of a face such as an eye, eyelid, and lip where the shading cues are distinctive compared to neighboring image pixels, it may fail to reconstruct some locations with relatively small shading variations such as a cheek. This problem is directly related to the estimated albedo which is highly biased to the luminance of the input image. In general, the estimation of the albedo is conducted with a given shape and the lighting representation which consists of DC (ambient) and single directional (diffuse) terms. If the ambient term, which is irrelevant to the shape, is estimated to have a relatively larger value than the diffuse term, the shading variation would be factorized into the albedo so that the estimated albedo would have the same value as in an image. Thus, the SfS error between the back-projected image and the input image would be minimized regardless of the geometric deformation. It is extremely challenging to estimate the correct albedo in an image with approximated lighting and geometry. To address this problem, some previous works adopted a statistical prior albedo built from hundreds of facial scan data. One may estimate the albedo by directly computing the appropriate parameters for the model [22] or use its mean albedo in regularization [23].

Inspired by these works, we combine the aforementioned approaches by optimizing the parameters of the prior albedo and apply it to the albedo estimation step as a regularizer. We observe that the optimized prior albedo can appropriately capture the true albedo rather than using the mean albedo directly in regularization. In addition, we propose a weighting strategy for albedo estimation based on chromaticity of the input facial image. Assuming that the similar albedos share similar chromaticity as well, the chromaticity value can provide evidence whether the pixel with similar albedo is shaded or not. By applying the proposed robust albedo estimation technique, we develop a 3D face reconstruction framework. In our framework, for a given image and optimized prior albedo,

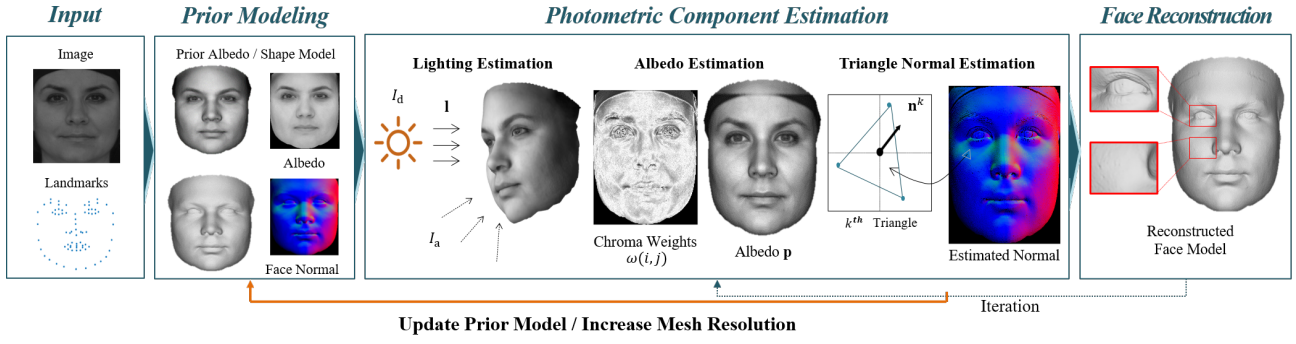


Fig. 2: An overview of the proposed 3D face reconstruction and photometric components estimation including the robust albedo estimation of a face.

the 3D face including shape and texture is reconstructed by computing the lighting parameters, albedo, and normal. Finally, the 3D facial shape is reconstructed by using the tetrahedron-based deformation from a prior shape model [24]. As shown in Fig. 1, our method can generate a detailed 3D face from an image such as wrinkle and pore in a face.

II. METHODS

An overview of our 3D facial shape recovery framework is shown in Fig. 2. At first, we compute the initial prior shape and albedo model from a given image with estimated landmarks by using 3DMM (Section. II-A). After computing the prior face model, we iteratively recover the geometry of a face as well as lighting parameters, albedo, and triangle normals (Section. II-C). The 3D facial geometry is reconstructed based on the rotation between a triangle normal of the previous step and the prior shape model by applying a tetrahedron-based deformation [24]. In addition, to capture the whole frequency features, we adopt a coarse-to-fine scheme by using Loop subdivision [25] as in [19].

A. Prior Face Modeling

We compute the prior face model including shape model and optimized albedo map with initial lighting parameters. To compute the initial prior face shape model, the pose, expression, and identity parameters of the shape model of the 3DMM are computed from given facial landmarks. Because the template-based SfS method is sensitive to the initial alignment, we apply the landmark-driven 3D warping method [19] to the points along with the eye, nose, and lip. For robust albedo estimation, we optimize the albedo parameters of the 3DMM by using roughly estimated lighting with mean albedo and fitted shape model [14]. By using the optimized parameters, we generate the initial prior albedo map for photometric component estimation.

B. Photometric Model of Face

As the face can be viewed as a diffuse reflector, we assume that the irradiance of the face follows the Lambertian reflectance model. Under this assumption, the intensity of each pixel (i, j) in the face region Ω of an luminance image I'

generated by back-projecting the facial shape with M vertices $\mathbf{X} \in \mathbb{R}^{3 \times M}$ and albedo $\mathbf{p} \in \mathbb{R}^M$ can be expressed as

$$\mathbf{I}'_{i,j} = \rho_{t_{i,j}} (I_a + I_d \max(0, \mathbf{n}^T_{t_{i,j}} \mathbf{l})), \quad (1)$$

where I_a , I_d , ρ , and $\mathbf{n} \in \mathbb{R}^3$ are the ambient light intensity, the diffuse light intensity with direction of $\mathbf{l} = [l_x, l_y, l_z] \in \mathbb{R}^3$, and the albedo and normal vector of the triangle $t_{i,j}$ projected on the pixel (i, j) . The face region, as well as the corresponding triangle of the face model for each pixel, can be computed by using z-buffering. Then, the albedo $\rho_{t_{i,j}}$ and normal vector $\mathbf{n}_{t_{i,j}}$ of the 3D face model can be computed by using

$$\rho_{t_{i,j}} = c_1^{t_{i,j}} \mathbf{p}_1^{t_{i,j}} + c_2^{t_{i,j}} \mathbf{p}_2^{t_{i,j}} + c_3^{t_{i,j}} \mathbf{p}_3^{t_{i,j}}, \quad (2)$$

$$\mathbf{n}_{t_{i,j}} = \frac{(\mathbf{x}_2^{t_{i,j}} - \mathbf{x}_1^{t_{i,j}}) \times (\mathbf{x}_3^{t_{i,j}} - \mathbf{x}_1^{t_{i,j}})}{\|(\mathbf{x}_2^{t_{i,j}} - \mathbf{x}_1^{t_{i,j}}) \times (\mathbf{x}_3^{t_{i,j}} - \mathbf{x}_1^{t_{i,j}})\|_2}, \quad (3)$$

where $(\mathbf{x}_1^{t_{i,j}}, \mathbf{x}_2^{t_{i,j}}, \mathbf{x}_3^{t_{i,j}})$ and $(\mathbf{p}_1^{t_{i,j}}, \mathbf{p}_2^{t_{i,j}}, \mathbf{p}_3^{t_{i,j}})$ represent the vertex coordinates and albedo values of a triangle corresponds to the pixel (i, j) , respectively; $(c_1^{t_{i,j}}, c_2^{t_{i,j}}, c_3^{t_{i,j}})$ are the barycentric coordinate weights computed by using z-buffer algorithm.

C. Chromaticity Weighted Photometric Component Estimation

To reconstruct a 3D face model from a single image, the photometric components including the lighting parameters, albedo, and normal maps are needed. To this end, we estimate these by minimizing the following objective function

$$E_I(\mathbf{p}, \mathbf{N}, \mathbf{I}') = \sum_{(i,j) \in \Omega} \omega_{i,j} (\mathbf{I}_{i,j} - \mathbf{I}'_{i,j})^2, \quad (4)$$

where \mathbf{N} , \mathbf{I}' , and $\mathbf{I}_{i,j}$ are the triangle normals, the lighting parameters defined as $\mathbf{I}' = [I_a, I_d, \mathbf{l}^T]$, and the luminance value of the input grayscale image, respectively. To reduce the inevitable errors related to misalignment of shape model and intrinsic albedo variation including skin spot or facial makeup, we introduce the weight $\omega_{i,j} \in [0, 1]$ for each pixel (i, j) . Inspired by the regularization strategy proposed in [21], $\omega_{i,j}$ is defined by the chromaticity value of the pixel location,

$$\omega_{i,j} = \phi \left(\left\| \frac{\mathbf{C}_{i,j}}{\mathbf{I}_{i,j}} - \frac{\mathbf{C}_{i,j}}{\mathbf{I}'_{i,j}} \right\|_2 \right), \quad (5)$$



Fig. 3: From left to right: input RGB image \mathbf{C} , back-projected image \mathbf{I}' , and pixel-wise weight $\omega_{i,j}$ by (5).

where \mathbf{C} is a RGB image and $\phi(x) = 1/(1 + \alpha \cdot x)^3$ is a robust kernel which is parameterized by user-defined constant α . As shown in Fig. 3, the regions within soft shadows and different albedo have smaller weights than others. Thus, the energy related to the pixel with different albedo has less effect than the others.

D. Iterative Optimization

Since jointly optimizing all of the unknown parameters in (4) is intractable, we separate the problem into estimating the lighting parameters, vertex albedo, and triangle normal in an iterative manner. After the photometric components are estimated, the 3D shape is computed by using tetrahedron-based deformation of the shape model at the iteration to the computed triangle normals. In the following, we describe the details of estimating each photometric component.

The lighting parameter \mathbf{l}' is estimated by solving $E_{\mathbf{l}}(\mathbf{l}'; \mathbf{p}^0, \mathbf{N}^0)$ where \mathbf{p}^0 and \mathbf{N}^0 are the given albedo and triangle normals of the prior face model respectively. Because of the max function in (1), this problem is a non-linear least square optimization. Since there are only 5 parameters to estimate, the Gauss-Newton solver can efficiently solve this problem in negligible time.

The vertex albedo \mathbf{p} is computed from given \mathbf{l}' and \mathbf{N}^0 after lighting parameters are estimated. We combine $E_{\mathbf{l}}$ with the additional regularization term to enforce smoothness of the vertex albedo along with the shape model. The objective function of vertex albedo optimization is

$$E_{\mathbf{p}}(\mathbf{p}; \mathbf{l}', \mathbf{N}^0) = E_{\mathbf{l}}(\mathbf{p}, \mathbf{l}', \mathbf{N}^0) + w_L \|\mathbf{Lp}^0 - \mathbf{Lp}\|_2^2, \quad (6)$$

where w_L and \mathbf{L} are the regularization weight and the uniform surface Laplacian matrix [26], respectively. Since the prior albedo is computed from the distribution of human face based on 3DMM, the additional term regularizes the deviation of estimated albedo from optimized prior. The minimization problem of (6) can easily be solved by using the linear least-square solver.

The triangle normal \mathbf{N} is computed by using previously estimated lighting parameters \mathbf{l}' and vertex albedo \mathbf{p} . Since there is only one constraint (luminance) given for each pixel, solely minimizing $E_{\mathbf{l}}$ may result in a degenerate solution. To avoid this, we add normal stabilization and smoothness constraints on the estimated triangle normal. The objective function of triangle normal estimation is defined as

$$E_{\mathbf{N}}(\mathbf{N}; \mathbf{N}^0, \mathbf{p}, \mathbf{l}') = E_{\mathbf{l}}(\mathbf{p}, \mathbf{N}, \mathbf{l}') + w_n \|\mathbf{N} - \mathbf{N}^0\|_2^2 + w_s \|\mathbf{HN}\|_2^2, \quad (7)$$

where w_n , w_s , and \mathbf{H} are normal stabilization, smoothness weight, and graph Laplacian matrix defined by using triangle connective of i^{th} triangle $\mathcal{N}_f(i)$ expressed as

$$\mathbf{H}_{i,j} = \begin{cases} -1 & \text{if } i = j, \\ \frac{1}{|\mathcal{N}_f(i)|} & \text{if } j \in \mathcal{N}_f(i), \\ 0 & \text{otherwise.} \end{cases} \quad (8)$$

The normal stabilization term in the middle of (7) penalizes the deviation of \mathbf{N} from the triangle normal of the prior shape model. Combined with the smoothness term $\|\mathbf{HN}\|$ in (7), it regularizes the smoothness of the estimated normal along with the neighboring triangle. The minimization of (7) is also a non-linear least square problem due to the max function in (2) and it is intractable to solve it for the whole triangle faces. Thus, we relax the problem by replacing the max function with indicator variable $d_{t_{i,j}}$. By using the indicator variable, the formula (2) can be rewritten as

$$\mathbf{I}''_{t_{i,j}} = \rho_{t_{i,j}} \left(\mathbf{I}_a + \mathbf{I}_d \left(d_{t_{i,j}} \mathbf{n}_{t_{i,j}}^T \mathbf{l} \right) \right), \quad (9)$$

where the indicator variable $d_{t_{i,j}}$ is defined by prior triangle normal

$$d_{t_{i,j}} = \begin{cases} 1 & \text{if } \mathbf{n}_{t_{i,j}}^0 \cdot \mathbf{l} \geq 0, \\ 0 & \text{otherwise.} \end{cases} \quad (10)$$

By substituting the \mathbf{I}' to \mathbf{I}'' of (3) in $E_{\mathbf{N}}(\mathbf{N}; \mathbf{N}^0, \mathbf{p}, \mathbf{l}')$, the problem can be converted into a linear least square problem. The normal for each triangle can be effectively computed by solving the linear least-square equation.

III. EXPERIMENTS

In this section, we present our comprehensive experimental results. As a prior face model, we used the Basel Face Model (BFM) [27] which is a generally adopted statistical parametric model for the shape and albedo of a face. The initial prior model is estimated by using the method in [5] with detected landmarks from [28]. In the photometric components estimation along with surface deformation, three iterations

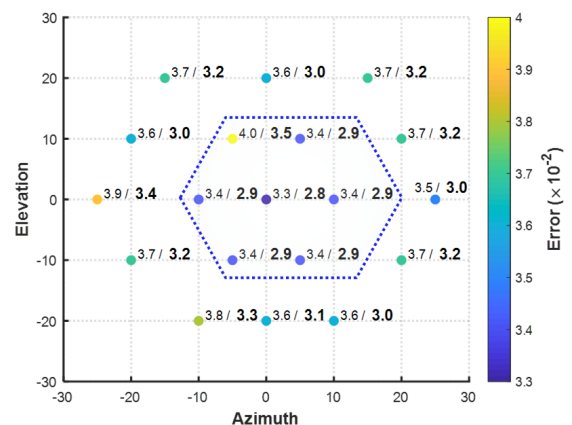


Fig. 4: The mean error measure of albedo estimation with different angles of light directions by using *mean / optimized prior model*, respectively.

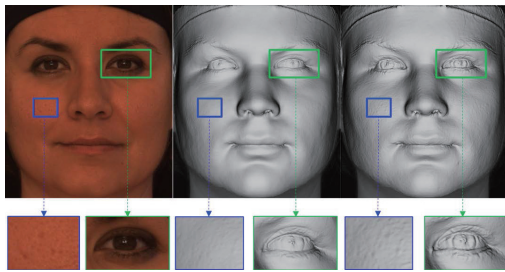


Fig. 5: Comparison of the reconstruction without (Middle) or with chromaticity weight (Right) of an input image (Left).

are enough to recover the 3D facial shape. At the end of each iteration, we apply the subdivision algorithm to the recovered 3D facial shape and update the facial prior model with computed shape and albedo.

We tested our robust albedo estimation method on images taken from the YaleB face dataset [30]. For each subject, we compute the ground truth albedo by using the given ambient intensity image and the direction of a light source for each image by using the Lambertian reflectance model. To compare the effect of using the optimized prior albedo with mean albedo, we estimate the albedo of each image of the dataset by the methods in Section. II-C. For 40 subjects, we analyzed the estimation error of an albedo with respect to an angular displacement of light direction in azimuth and elevation within 40 degrees. As shown in Fig. 4, the estimation error of albedo has a lower value with optimized prior albedo than mean albedo. To clarify the performance gain of the proposed method, we further draw the table for average error inner (inside the dotted line in Fig. 4) and outer angles in Table I. Comparing the average error between the inner and outer angles, the error of the proposed method deviates smaller while the error of the mean prior albedo-based method largely increases.

To demonstrate the quality of our 3D facial shape reconstruction framework, we tested it using the Bosphorus dataset [29] which provides structured-light scanned 3D point clouds of a face with 105 subjects, as well as a corresponding single RGB image. Note that, the SfS based method without any metric information such as the correct depth value of boundary points, the error estimation by using mean squared error (MSE) is not convincing. Furthermore, the scanned point clouds in the dataset are quite noisy making the quantitative

TABLE I: Comparison of error between the inner and outer angles (mean±std.). In the third column, we show the difference of mean errors between inner and outer angles (scaled by 10^{-2}).

	Inner angles	Outer angles	Outer-Inner
Mean prior	3.4714 ±0.2360	3.6750 ±0.1055	0.2036
Optimized prior	2.9700 ±0.2273	3.1396 ±0.1047	0.1696

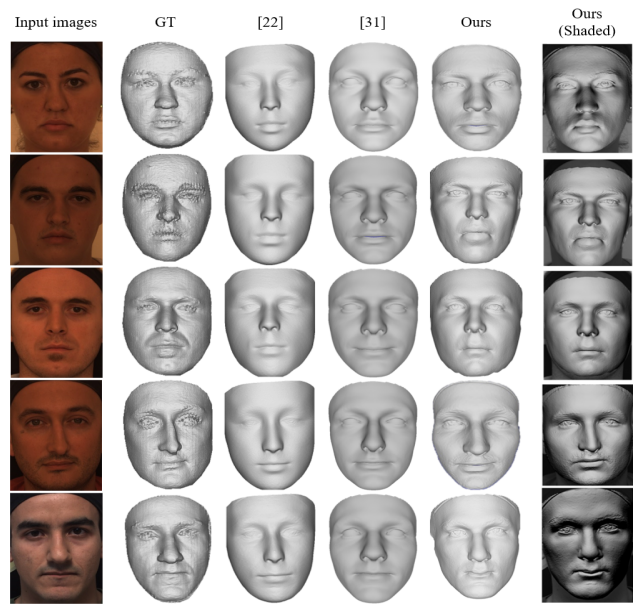


Fig. 6: 3D Face reconstruction results of images from Bosphorus dataset. (Left to Right) The ground truth, the result of the method [22], [31], and our method are presented. We also show the back-projected 3D face to each input image with computed lighting.

measurement skeptical. Therefore, we omitted the quantitative measure for this reason. In Fig. 5, the effect of chromaticity-based weight for 3D facial shape reconstruction is shown. Since the proposed weight prevents the albedo to be factored into the shading, we can observe that the facial details around cheek and eye regions are much-enhanced. Note that we only applied this weight to the albedo estimation step. In addition, we illustrate the 3D face reconstruction result by using the proposed method and recently proposed methods [22], [31] for 5 samples in the Bosphorus dataset in Fig. 6. Compared to the proposed method, the result from [22] exhibits an oversmoothed appearance compared to ours. As mentioned, it is caused by the albedo estimation without an appropriate prior albedo. On the other hand, the proposed framework is able to recover high-quality geometric details including pores.

IV. CONCLUSION

We presented a 3D facial shape recovery framework from a single image with a robust albedo estimation method. From the prior face model including shape and albedo, our framework iteratively reconstructs the 3D facial shape with lighting, albedo, and normal estimation. Incorporating the optimized albedo prior as well as chromaticity to the single image-based 3D shape recovery process allows the method to enhance the detail parts of the face while preventing noisy deformations. In the experiments, we have shown that our framework is capable of reconstructing a facial with highly enhanced details.

ACKNOWLEDGMENT

This work was supported by Korea Evaluation Institute of Industrial Technology (KEIT) grant funded by the Korea government (MOTIE) (No. 20012603, Development of Emotional Cognitive and Sympathetic AI Service Technology for Remote (Non-face-to-face) Learning and Industrial Sites).

REFERENCES

- [1] T. Hassner *et al.*, "Pooling faces: template based face recognition with pooled face images," *Proc. IEEE Comput. Soc. Conf. Comput. Vis. Pattern Recognit. Workshop (CVPRW)*, Jun. 2016, pp. 59-67.
- [2] G. Hu *et al.*, "Face recognition using a unified 3d morphable model," *Proc. Eur. Conf. Comput. Vis. (ECCV)*, Oct. 2016, pp. 73-89.
- [3] J. Park, S. Heo, K. Lee, H. Song, and S. Lee, "Robust Facial Pose Estimation Using Landmark Selection Method for Binocular Stereo Vision," *Proc. IEEE Int. Conf. Image Process. (ICIP)*, Oct. 2018, pp. 186-190.
- [4] T. Choi, J. Kang, H. Song and S. Lee, "Fitting Facial Models to Spatial Points: Blendshape Approaches and Benchmark," *Proc. IEEE Int. Conf. Image Process. (ICIP)*, Oct. 2018, pp. 2650-2654.
- [5] X. Zhu, Z. Lei, J. Yan, D. Yi, and S. Z. Li, "High-fidelity pose and expression normalization for face recognition in the wild," *Proc. IEEE Int. Conf. Comput. Vis. Pattern Recognit. (CVPR)*, Jun. 2015, pp. 787-796.
- [6] B. Kwon, J. Huh, K. Lee, and S. Lee, "Optimal Camera Point Selection toward the Most Preferable View of 3D Human Pose," *IEEE Trans. Syst. Man Cybern. Syst.*, in press.
- [7] K. Lee, I. Lee, and S. Lee, "Propagating LSTM: 3D Pose Estimation based on Joint Interdependency," *Proc. Eur. Conf. Comput. Vis. (ECCV)*, Sep. 2018, pp. 119-135.
- [8] C. Cao, Q. Hou, and K. Zhou, "Displaced dynamic expression regression for real-time facial tracking and animation," *ACM Trans. Graph. (TOG)*, vol. 33, no. 4, pp. 1-10, Jul. 2014.
- [9] J. Kang and S. Lee, "A Greedy Pursuit Approach for Fitting 3D Facial Expression Models," *IEEE Access*, vol. 8, pp. 192682-192692, Oct. 2020.
- [10] W. Kim, S. Lee, and A. C. Bovik, "VR Sickness versus VR Presence: A Statistical Prediction Model," *IEEE Trans. Image Process.*, vol. 30, pp. 550-571, Nov. 2020.
- [11] J. Kim, W. Kim, H. Oh, S. Lee, and S. Lee, "A Deep Cybersickness Predictor based on Brain Signal Analysis for Virtual Reality Content," *Proc. Int. Conf. Comput. Vis. (ICCV)*, Nov. 2019, pp. 10580-10589.
- [12] V. Blanz and T. Vetter, "Face recognition based on fitting a 3D morphable model," *IEEE Trans. Pattern Anal. Mach. Intell.*, vol. 25, no. 9, pp. 1063-1074, Sep. 2003.
- [13] O. Aldrian and W. A. Smith, "Inverse rendering of faces with a 3D morphable model," *IEEE Trans. Pattern Anal. Mach. Intell.*, vol. 35, no. 5, pp. 1080-1093, May. 2013.
- [14] J. Booth *et al.*, "3D face morphable models "in-the-wild"," *Proc. IEEE Int. Conf. Comput. Vis. Pattern Recognit. (CVPR)*, Jul. 2017, pp. 48-57.
- [15] J. Kang, S. Lee, and S. Lee, "Competitive Learning of Facial Fitting and Synthesis Using UV Energy," *IEEE Trans. Syst. Man Cybern. Syst.*, in press.
- [16] H. Song, J. Park, S. Heo, J. Kang, and S. Lee, "PatchMatch based Multiview Stereo with Local Quadric Window," *Proc. ACM Int. Conf. Multimed.*, Oct. 2020, pp. 2664-2672.
- [17] A. D. Nguyen, S. Choi, W. Kim, and S. Lee, "GraphX-convolution for point cloud deformation in 2D-to-3D conversion," *Proc. Int. Conf. Comput. Vis. (ICCV)*, Nov. 2019, pp. 8628-8637.
- [18] X. Cao *et al.*, "Sparse Photometric 3D Face Reconstruction Guided by Morphable Models," *Proc. IEEE Int. Conf. Comput. Vis. Pattern Recognit. (CVPR)*, Jun. 2018, pp. 4635-4644.
- [19] J. Roth, Y. Tong and X. Liu, "Adaptive 3D face reconstruction from unconstrained photo collections," *Proc. IEEE Int. Conf. Comput. Vis. Pattern Recognit. (CVPR)*, Jun. 2016, pp. 4197-4206.
- [20] F. Langguth, K. Sunkavalli, S. Hadap, and M. Goesele, "Shading-aware multi-view stereo," *Proc. Comput. Vis. ECCV*, Oct. 2016, pp. 469-485.
- [21] M. Zollhöfer *et al.*, "Shading-based refinement on volumetric signed distance functions," *ACM Trans. Graph. (TOG)*, vol. 34, no. 4, pp. 1-14, Jul. 2015.
- [22] L. Jiang, J. Zhang, B. Deng, H. Li and L. Liu, "3D face reconstruction with geometry details from a single image," *IEEE Trans. Image Process.*, vol. 27, no. 10, pp. 4756-4770, Jun. 2018.
- [23] I. Kemelmacher-Shlizerman and R. Basri, "3D face reconstruction from a single image using a single reference face shape," *IEEE Trans. Pattern Anal. Mach. Intell.*, vol. 33, no. 2, pp. 394-405, Feb. 2011.
- [24] S. Heo, H. Song, J. Kang and S. Lee, "Local spherical harmonics for facial shape and albedo estimation," *IEEE Access*, vol. 8, pp. 1777424-1777436, Sep. 2020.
- [25] C. Loop, "Smooth subdivision surfaces based on triangles," *Master's thesis, University of Utah, Department of Mathematics*, 1987.
- [26] A. Nealen, T. Igarashi, O. Sorkine, and M. Alexa, "Laplacian mesh optimization," *Proc. ACM GRAPHITE.*, pp. 381-389, Nov. 2006.
- [27] P. Paysan, R. Knothe, B. Amberg, S. Romdhani, and T. Vetter, "A 3D face model for pose and illumination invariant face recognition," *Proc. IEEE Int. Conf. Adv. Video Signal Based Surveillance*, pp. 296-301, Sep. 2009.
- [28] H. Song, J. Kang, and S. Lee, "ConcatNet: A Deep Architecture of Concatenation-Assisted Network for Dense Facial Landmark Alignment," *Proc. IEEE Int. Conf. Image Process. (ICIP)*, Oct. 2018, pp. 2371-2375.
- [29] A. Savran *et al.*, "Bosphorus database for 3D face analysis," *European Workshop on Biometrics and Identity Management*, pp. 47-56, Dec. 2008.
- [30] A. S. Georghiadis, P. N. Belhumeur, and D. J. Kriegman, "From few to many: Illumination cone models for face recognition under variable lighting and pose," *IEEE Trans. Pattern Anal. Mach. Intell.*, vol. 23, no. 6, pp. 643-660, Jun. 2001.
- [31] Y. Deng *et al.*, "Accurate 3D face reconstruction with weakly-supervised learning: From single image to image set," *Proc. IEEE Comput. Soc. Conf. Comput. Vis. Pattern Recognit. Workshop (CVPRW)*, Jun. 2019.